Bioorganic & Medicinal Chemistry 20 (2012) 1354–1363

Contents lists available at SciVerse ScienceDirect

Bioorganic & Medicinal Chemistry

journal homepage: www.elsevier.com/locate/bmc

Novel indoleamine 2,3-dioxygenase-1 inhibitors from a multistep in silico screen

Jason R. Smith [a], Krystal J. Evans [b,†], Adam Wright [b], Robert D. Willows [a], Joanne F. Jamie [a,b,*,‡], Renate Griffith [b,c]

[a] Department of Chemistry and Biomolecular Sciences, Macquarie University, Sydney, NSW 2109, Australia
[b] School of Chemistry, University of Wollongong, Wollongong, NSW 2500, Australia
[c] School of Medical Sciences/Pharmacology, University of New South Wales, Sydney, NSW 2052, Australia

ARTICLE INFO

Article history:
Received 3 August 2011
Revised 15 October 2011
Accepted 22 October 2011
Available online 30 October 2011

Keywords:
IDO inhibitors
Heme
Computer-aided drug design
Pharmacophore
Docking

ABSTRACT

Indoleamine 2,3-dioxygenase-1 (IDO-1) is a heme containing enzyme that catalyses the initial step in the major pathway of L-tryptophan catabolism; the kynurenine pathway. A large body of evidence has been accumulating for its immunosuppressive and tumoural escape roles and its applicability as a therapeutic target. Of particular interest is the possibility that IDO-1 inhibition may arrest, and sometimes revert, tumour growth. There exists a continuing need for the development of new and specific inhibitors for IDO-1, and we have created three pharmacophores designed to aid in this search. Initial database hits were further screened using Kier flexibility and a 'What-If' docking technique, designed to overcome the inherent limitations of today's forcefields with regards to heme chemistry. Eighteen compounds were tested in vitro, yielding four novel inhibitors with low micromolar IC_{50} values, comparable with current inhibitors.

1. Introduction

Indoleamine 2,3-dioxygenase (IDO-1) is a heme containing enzyme responsible for the initial step in the major pathway of L-tryptophan catabolism, the kynurenine (Kyn) pathway. IDO-1 is a monomer active in the ferrous (Fe^{2+}) form, but is easily autooxidised to the inactive ferric (Fe^{3+}) form.[1] Two other enzymes capable of performing the same reaction exist in the paralogue IDO-2, and tryptophan 2,3-dioxygenase (TDO).[2] The active sites of each bear a striking resemblance but differ in their kinetics and substrate specificities.[3,4] These enzymes are unique in being the only examples of heme containing dioxygenases known in humans.[5] Mechanistically these enzymes remain an enigma, and although much work has been done to identify intermediates, they remain elusive.[1,6,7] An in vivo reduction system has yet to be identified for IDO-1, although in vitro a number of systems have been used such as methylene blue/ascorbic acid. Most interesting in this regard is the use of cytochrome P450 reductase in combination with cytochrome b_5, giving sigmoidal kinetics.[8] This suggests the presence of a heterocomplex between IDO-1 and cytochrome b_5 under experimental conditions.

The crystal structure (PDB: 2D0T) was released in 2006 as a cross-linked dimer, minus an unresolved loop containing residues 360–380.[9] Co-crystalised ligands were 4-phenylimidazole (PI) and two buffer molecules of 2-(*N*-cyclohexylamino)ethane sulfonic acid (CHES) (Fig. 1). The active site is primarily hydrophobic in nature, with the exception of Ser167 at the rear of the pocket and Arg231 and the 7-propanoate arm of heme to either side of the entrance. A highly conserved flexible loop (260–265) is also important for binding and conformational flexibility.

A large body of evidence has been accumulating for IDO-1's immunosuppressive and tumoural escape roles and it's applicability as a therapeutic target.[10–12] Inhibition of IDO-1 via small molecules has lead to the arrest or reversion of tumour growth in animal systems.[12] Although a number of inhibitor scaffolds have been identified, many of these inhibitors possess relatively few specific interactions with IDO-1, relying primarily on heme ligation.[13–15] To date only two molecules have achieved phase 1 clinical testing, 1-methyl-D-tryptophan (D-1MT, NewLink Genetics) and an undisclosed molecule of the hydroxylamidine series

Abbreviations: IDO-1, indoleamine 2,3-dioxygenase-1; rhIDO-1, recombinant human IDO-1; PI, phenylimidazole; CHES, 2-(*N*-cyclohexylamino)ethane sulfonic acid; D-1MT, 1-methyl-D-tryptophan; L-1MT, 1-methyl-L-tryptophan; DS, Discovery Studio 2.5; MOE, Molecular Operating Environment; HBA, hydrogen bond acceptor; HBD, hydrogen bond donor; RA, aromatic ring; Hyd, hydrophobic; +ve, positive ionisable.

* Corresponding author: Tel.: +61 2 9850 8283; fax: +61 2 9850 8313.
E-mail address: joanne.jamie@mq.edu.au (J.F. Jamie).
† Present address: Walter and Eliza Hall Institute, Parkville, Victoria 3050, Australia.
‡ Present address: Department of Chemistry and Biomolecular Sciences, Macquarie University, Sydney, NSW 2109, Australia.

0968-0896/$ - see front matter © 2011 Elsevier Ltd. All rights reserved.
doi:10.1016/j.bmc.2011.10.068

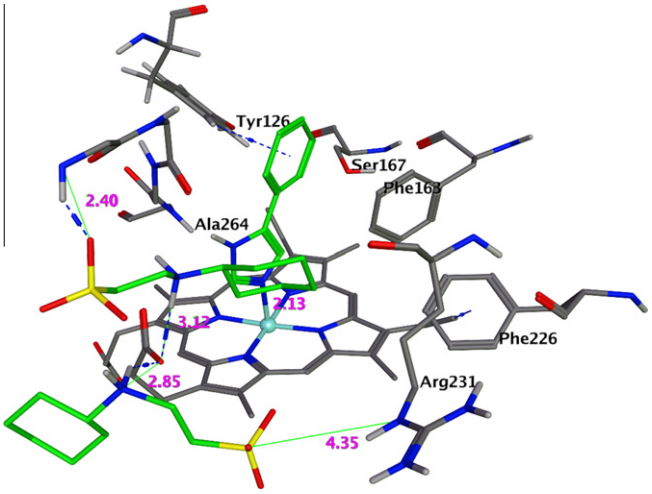

Figure 1. The crystal structure of recombinant human IDO-1 (rhIDO-1, PDB: 2D0T).[9] Co-crystalised ligands are shown with green carbons and important active site residues are labelled. Heavy atom distances are given in pink. Atom colours: grey–carbon, yellow–sulfur, dark blue–nitrogen, red–oxygen, light blue–iron, white– hydrogen. Non-polar hydrogens have been omitted for clarity. Note that the hydroxyl group of Tyr126 is not accessible for ligand binding in the current crystal structure.

(INCB024360, Incyte) (clinical trial numbers NCT00739609 and NCT01195311, respectively).[16] Therefore, there exists a continuing need for the development of new IDO-1 inhibitors.

The aim of this work was to utilise multiple pharmacophores in conjunction with docking techniques to perform in silico screening for new IDO-1 inhibitors. This involved searching for new 'core' scaffolds (small, rigid molecules) that could later be modified for increased interaction with the active site. In parallel, we searched for larger, 'extended' molecules, capable of interacting with Ser167, Arg231 and/or the propanoate arm of heme, under the assumption that these interactions may define an IDO-specific pharmacophore.

2. Materials and methods

Default parameters were used for all computational procedures unless otherwise stated. The CHARMM22 forcefield (as implemented in Molecular Operating Environment version 2008.10 (MOE, Chemical Computing Group, Montreal, Canada)) was used for all molecular mechanics techniques, with the Born solvation model unless otherwise stated. Dielectric constants were 4 inside the protein and 80 in the solvent. Van der Waals forces used the Lennard–Jones 12-6 potential with a 10 Å cutoff. Energy minimisations automatically switched between steepest decent, conjugate gradient and truncated Newtonian methods, depending on the size of the energy gradient. All distances and root mean square deviations (RMSD) given are heavy atom distances in angstroms.

2.1. Creation of ligand-based pharmacophore

Pharmacophore modelling was carried out in Discovery Studio 2.5 (DS, Accelrys, California, USA). Data sets were created through a comprehensive literature search of known IDO-1 inhibitors. In house data of three novel 3-amino-2-naphthoic acid analogues was also used. Ideally, scaffolds in the training set displayed a varied SAR, with good diversity in structure and spread of activities.

The feature set contained in the molecules led us to choose the following features for pharmacophore elucidation; H-bond acceptor (HBA), H-bond donor (HBD), aromatic ring (RA), hydrophobic (Hyd) and positive ionisable (+ve) (a group either in its cationic form or capable of existing in a cationic form). Conformations were generated in DS using the Best method, as recommended for pharmacophores. Pharmacophore hypotheses were generated using the 3D QSAR Pharmacophore Generation protocol. The minimum number of features was changed from 1 to 3, minimum interfeature distance was changed from 2.97 to 2 Å, and the maximum number of excluded volumes was changed from 0 to 5.

2.2. Creation of receptor-based pharmacophores

Two receptor-based pharmacophores were created. The first was taken directly from chain A of the IDO-1 crystal structure (PDB: 2D0T[9]) and its co-crystalised ligands PI and two molecules of CHES. An HBA feature was centred at PI's ligating nitrogen and its lone-pair vector used for the HBA vector. An RA feature was centred at the centre of the benzene ring with its vector perpendicular to this plane. A +ve feature was centred on the nitrogen of the CHES molecule closest to the pocket (NHE502 in the PDB file). An HBA feature was centred on the sulfonic acid oxygen closest to Arg231 (NHE503 in the PDB file). Several lone-pair vectors were given by DS to choose from for this feature. The vector most directly pointing toward the guanidinium group of Arg231 was used. Tolerance sphere radii, specifying the volume in which a feature can be satisfied by an atom or group of atoms, were of default size: 1.6 Å for HBA, HBD, RA and +ve features of the ligand, 1.6 Å for an RA vector end point, and 2.2 Å for HBA and HBD vector end points. These vector end points approximate the locations of interacting features on the protein. Excluded volumes were placed around receptor atoms within 4 Å of the above feature's centres and given the default 1.2 Å tolerance radius. Excluded volumes around the three carboxylate atoms of heme were removed to simulate the flexibility of this group. Additional and unnecessary excluded volumes were manually removed so as to still form a representation of the pocket's surface, whilst reducing database search time.

A second structure-based pharmacophore was generated from the docking of *S*-(4-chlorobenzyl)isothiourea (see section 2.5 for docking methods). An RA feature was created as above using the benzene carbons. The +ve feature was created at the centroid of the two nitrogen atoms and the HBA feature centred at the sulfur atom; its vector given by the positioning of the Fe atom of heme. Excluded volumes and tolerance spheres were created as above.

2.3. Validation of hypotheses

Hypotheses were validated by looking at the correlation co-efficient between predicted and actual activities of the training set, a cost value analysis, as well as Fischer randomisaton as implemented in DS.

In the cost value analysis the difference between the total cost of the hypothesis and the null cost of the training set is known as the null difference. A null difference of 40 bits or more is indicative of the hypothesis being statistically non-random. A configuration cost of the training set is also given. A configuration of 17 or more indicates that the software was not able to consider all possible configurations of the training set.

Fischer randomisation randomly reassigns activity data to molecules of the training set, and then generates new hypotheses from these datasets. These random hypotheses should have correlations and a total cost lower than that of the hypothesis of the original training set. The confidence interval chosen was 90%.

We also tested the predictiveness of the final model against a dataset of known IDO-1 inhibitors. The Ligand Pharmacophore Mapping protocol was used to predict the activities of the test set. The mapping method was changed from rigid to flexible for this procedure with a maximum of one omitted feature.

2.4. Database searching

The Maybridge Screening Collection database as implemented in DS (59,652 molecules) was searched with the pharmacophores utilising the Best method and all hits were kept for further consideration. Based on IDO-1 inhibitors such as PI, 1,4-naphthoquinone, 3-amino-2-naphthoic acid, benzothiazolethione and phenylmethanthiol,[13,15,17,18] we first narrowed the list down to molecules containing potential heme ligators through the use of SMARTS-like strings in the MOE interface. Strings used were: aromatic cyano (cC#N), carboxylic acid (C(=O)O[!a&!A]), quinone and its nitrogen analogue (C(=[N,O])C=CC(=[N,O])C=C), aryl thiols (a–S) and thione ([C,c]=S) structures, and heteroaromatic structures with an accessible lone pair (ca[!c]c), (ca[!c]a[!c]).[19] As the inhibitor scaffolds listed above are rigid molecules, we ranked hits based on their Kier flexibility score (as implemented in MOE) for 'cores'.[20] An 'extended' molecules list was also created by ranking hits on their fit to the pharmacophores. 73 of the best ranking molecules (34 cores, 39 extended) with diverse structures were then submitted to docking.

2.5. Docking

Docking was performed in MOE, which uses a molecular mechanics-based docking procedure. Random triplets of atoms from ligand conformations are aligned with random positions in the receptor. This then represents the initial pose and the procedure is repeated until the requested number of initial poses are found (we defined this number to be such that approximately two-thirds of the poses were duplicates, ensuring adequate sampling). Duplicate poses were discarded and the remaining were energy minimised to form final poses. Initially, 73 hit molecules were selected for coarse docking and minimised using the distance-dependent solvation model and grid-based electrostatics. Subsequently, 20 of these molecules were selected by manual inspection, in combination with scoring based on the pose's solvation energy (GB/VI scoring, as implemented in MOE), for full forcefield docking. During this manual inspection, we were specifically looking for molecules that fitted well into the aromatic binding cleft and had a potential interaction with the Fe of heme. For extended molecules, we wished to see the above, but also were looking for favourable interactions with Ser167, Arg231 and/or the propanoate arm of heme. Any new hits should not be closely related to known IDO-1 inhibitors.

Chain A of the IDO-1 crystal structure (PDB: 2D0T[9]) was used for all docking runs. Waters greater than 4.5 Å from the protein were removed before protons were added and the H-bonding network optimised using MOE's Protonate3D protocol. The active site was defined using dummy atoms created by MOE's Site Finder protocol where the connection distance was changed from 2.5 to 1.9 Å. This was done to confine the initial ligand placement more centrally to the heme. Initial ligand placement was performed using the Triangle Matcher algorithm.

During minimisation, sidechains of residues within 6 Å of the ligand were defined as flexible, whilst backbone atoms were fixed. No tethers were applied to flexible atoms. MOE automatically increases the 6 Å boundary if a final pose comes to within 80% of this cutoff distance. Gradient minimisation was performed to a root mean square gradient (RMSG, kcal/mol) of 0.01 (0.001 for poses making use of the potential explained below) or 500 iterations, whichever came first.

2.6. Use of a cubic potential penalty as a 'What-If' analysis

We applied a flat-bottomed cubic energy potential to ligands during final docking in order to perform a 'What-If' analysis of the compounds. That is, we assumed a particular atom ligated heme in order to see what the rest of the molecule might look like in such a situation. The potential was applied in the form of an energy penalty for Fe-ligand distances that were too large or small. The cubic energy potential was between the Fe atom of heme and a single ligand atom and takes the form of: $E = w(|r^2 - B^2|)^3$, where E is the energy to be added to the potential energy of the system, w is a weighting constant (20 kcal/mol), r is the current distance between the two restrained atoms and B is the distance boundary being violated. The flat-bottom boundaries for nitrogen and oxygen atoms were between 2.1–2.2 and 2.2–2.3 Å for sulfur. The potential is equal to zero at and in between these two boundary distances. These boundaries were based on the covalent radii of Fe–N/O/S complexes listed in the literature.[21]

2.7. Two dimensional similarity analyses

Similarity analyses were carried out by three different fingerprint methodologies. Fingerprints of each molecule were calculated using the MDL (Symyx) MACCS structural keys as well as two different three-point, two-dimensional, pharamcophore methods (GpiDAPH3 and TGT methods), as implemented in MOE. A Tanimoto co-efficient of 0.85 or greater was used to define molecules as similar.

2.8. Growth of IDO-1

Recombinant human IDO-1 (rhIDO-1) was grown as previously reported with slight modifications.[22] Briefly, *Escherichia coli* (EC538, pREP4, pQE9-IDO) was grown overnight on Luria Bertani (LB) agar (tryptone (2% w/v), yeast extract (1% w/v), bacteriological agar (1.5% w/v), NaCl (1% w/v), ampicillin (100 μg/mL) and kanamycin (50 μg/mL)) at 37 °C. A single colony was inoculated into 100 mL of liquid LB media containing ampicillin and kanamycin as above. This was then grown overnight at 30 °C. Three 20 mL aliquots were taken and added to three separate flasks containing 980 mL of liquid LB media and grown overnight at 18 °C to an $OD_{600\ nm}$ of 1.2. Each flask was then diluted with a further 600 mL of liquid LB media previously cooled to 18 °C. To each culture mix was added δ-aminolevulinic acid (500 μM final concentration) and incubated for a further 3 h at 18 °C. rhIDO-1 expression was induced by the addition of IPTG (100 μM). Incubation was continued at 18 °C for a further 4 days. Cultures were pelleted at 5,200*g* at 4 °C for 20 min and resuspended in ice-cold Tris–HCl buffer (25 mM, pH 7.4) containing $MgCl_2$ (10 mM), imidazole (10 mM), DNase (1 mg/L), EDTA-free cocktail inhibitors (Roche, 1 tab/L of culture), PMSF (5 M in isopropanol, final concentration 1 mM) and NaCl (150 mM) and lysed through an emulsifier at 15,000 psi, four times. The cell lysate was then centrifuged as above and the supernatant passed through a 5 mL nickel affinity HisTrap-FF column (GE healthcare) pre-equilibrated with ice-cold binding buffer. The binding buffer contained Tris–HCl (25 mM, pH 7.4), imidazole (10 mM), PMSF (5 M in isopropanol, final concentration 1 mM), NaCl (500 mM) and 0.1% v/v Tween-20. The column was then eluted with 20 mL of binding buffer, followed by 4 × 20 mL of ice-cold elution buffer. The elution buffer contained the above except Tween-20 was absent and imidazole concentration was 20, 30, 50 or 300 mM. The final 20 mL elution was then collected in 1 mL aliquots and the deepest red aliquots were combined and immediately buffer exchanged on a Nap-10 column (GE healthcare) with Tris-HCl (50 mM, pH 7.4) and concentrated with an Amicon Ultra centrifuge filter (30 kDa cutoff, Millipore, 5,200 g, 4 °C, 20 min) to give ~750 μL of red–black sample, which was then diluted 1:1 with 80% (v/v) glycerol (stored at −20 °C) and flash frozen in liquid nitrogen and stored at −80 °C.

Table 1
Inhibitor data used for pharmacophore creation

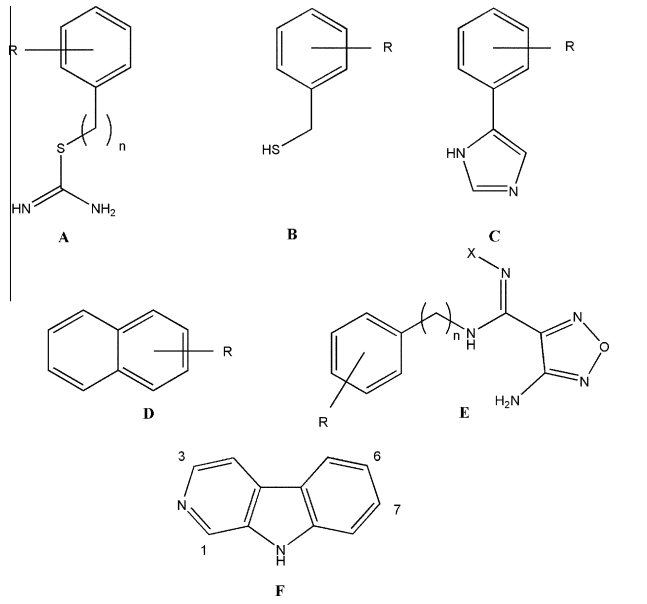

Scaffold	R, X, n	IC_{50}[a] (μM)
E	3-Cl, OH, *n* = 0	0.086[24]
B	3,4-diCl	0.1[17]
E	H, OH, *n* = 1	1.0[24]
E	3-Cl, H, *n* = 0	1.4[24]
E	3-*iso*propyl, OH, *n* = 0	2.1[24]
F	3*n*-butyl	3.3[25,b]
B	2,4-diCl	3.5[17]
C	2-OH	4.8[14]
E	4-Cl, OH, *n* = 0	6.0[24]
F	3-MeOOC-6-F	7.4[25,b]
D	2-COOH-3-NH_2	15[c]
C	1,5-diphenylimidazole	32[14]
F	3-NO_2	37[25,b]
C	—	48[14]
F	—	178[25,b]
D	3-CH_2OH-2-NH_2	190[c]
C	3-OH	370[14]
D	3-MeOOC-2-NH_2	460[c]
D	2-COOH-3-OH	1000[c]
C	4-OH	1200[14]
F	1-Me-7-OH	2000[26]
A	—, *n* = 1	61[17]
A	4-Cl, n = 2	57[17]
A	2-Cl, *n* = 1	10[17]
A	2,4-diCl, *n* = 1	0.4[17]

[a] With 200 μM L-tryptophan as substrate.
[b] K_i.
[c] This study.

2.9. Inhibition assays

Test compounds were purchased from Maybridge and used as received. For compounds that were unreactive towards Ehrlich's reagent, and did not absorb at 480 nm at tested concentrations, inhibition assays were performed as described previously.[23] For the remaining compounds, kynurenine levels were measured via HPLC. Supernatants (100 μL) were analysed on an analytical C18 column (Phenomenex Synergi Hydro-RP, 250 × 4.60 mm, 4 μm) fitted with a 3 mm C18 guard column. Analysis was performed isocratically utilising potassium phosphate buffer (10 mM, pH 7.0) with methanol (3% v/v) at 0.8 mL/min for 20 min. Kynurenine was measured by the absorbance at 224 nm.

All assays were performed in triplicate alongside controls devoid of IDO-1 as well as DMSO carrier controls. 1-Methyl-L-tryptophan (L-1MT) and norharman were used as positive controls. All tested compounds were stored in a DMSO stock solution (1:1 with water for L-1MT) and stored at −20 °C. Final DMSO concentrations where 0.5% v/v in the assay system. L-Tryptophan concentration was 200 μM. Holoenzyme concentration was ~8 nM (35 mg/mL at 100,000 fold dilution). Enzyme concentration was determined by its absorbance at 405 nm (25 mM Tris–HCl, pH 7.3 at 10 °C) using an extinction co-efficient of 159 mM^{-1} cm^{-1}.[24]

Table 2
Statistics of hypotheses created from training set 2.

Hypo	Total cost	Null difference	R	Features[b]	Excl. vols.
1	91	51	0.93	HBA, 2 × Hyd	4
2	98	44	0.88	HBA, 2 × Hyd, +ve	3
3	101	41	0.84	HBD, 2 × Hyd, RA	2
4	101	41	0.85	HBD, Hyd, RA	2
Random[a]	102		0.86		

[a] Refers to the highest ranked hypothesis output by the Fischer randomisation.
[b] HBA: hydrogen-bond acceptor. Hyd: hydrophobic. +ve: positive ionisable. HBD: hydrogen-bond donor. RA: aromatic ring.

3. Results and discussion

3.1. Training set creation

Training set molecules were chosen using the following criteria: (1) the scaffold's SAR series should have as much structural diversity as possible, as well as a diverse spread in inhibitory activity; (2) they should be known or suspected of ligating heme; (3) the total spread of activities for the training set should cover at least four orders of magnitude. The *S*-benzylisothioureas and phenylmethanthiols,[18] phenylimidazoles,[14] hydroxylamidines,[25] and β-carbolines[26,27] were all considered to satisfy the first criterion. The tryptophans and analogues,[4,17,28] brassinins[29] and naphthoquinones/indolequinones (and their nitrogen analogues)[13,15,30] also fit this criteria but were not considered. The tryptophans do not ligate heme, and therefore fail criterion 2.[31] Although there is some evidence that the brassinins ligate heme, they also display a good 3D overlay with tryptophan, and therefore may mimic it (Supplementary Fig. 1). Lastly, as the quinones and their analogues may have redox activity, they were excluded. We have also had interest in the aminonaphthoic acids since their first reporting in 1994 by Peterson et al.[17] The aminonaphthoic acids are not a well studied scaffold for IDO-1 inhibition, however, they show great promise, with 3-amino-2-naphthoic acid displaying 74% inhibition at 100 μM with 200 μM L-tryptophan.[17] Initially reported as a competitive inhibitor, our own spectroscopic investigations reveal that it distorts the heme in a manner similar to the β-carboline norharman (data not shown), known to ligate heme.[31] We therefore set about testing three additional aminonaphthoic acid analogues (Table 1). Synthetic procedures can be found in the Supplementary data.

The reported pK_a of *S*-methylisothiourea is 9.83, suggesting that a significant proportion of the compound should be protonated in the assay system (pH 6.5) and may not have a lone-pair available for heme ligation.[32] Additionally, the *N,N'*-dimethyl analogue still retains activity, and the authors suggested this as evidence against heme ligation, in light of its known carboxylate interaction ability.[18] We therefore tested the importance of the *S*-benzylisothioureas (scaffold A, Table 1) to the generated hypotheses by removing these from the training set, creating training set 2. The training set molecules are contained within Table 1 and cover five orders of magnitude in inhibitory activity.

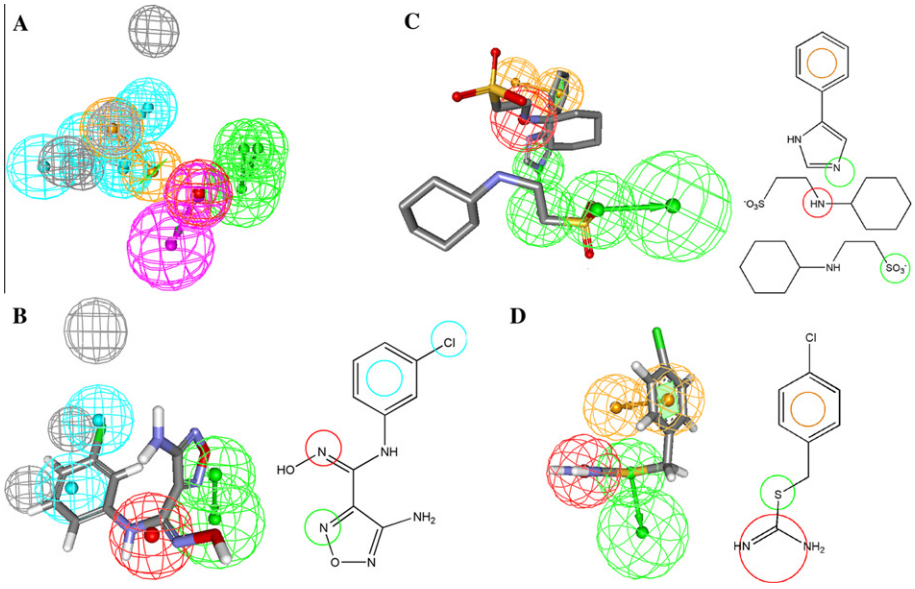

Figure 2. Pharmacophores in this study. (A) Overlay of hypotheses 1–4 from training set 2. (B) Hypothesis 2 from training set 2 mapped to most active inhibitor. (C) Receptor based pharmacophore from crystal strucutre. (D) Receptor based pharmacophore from docking of *S*-(4-chlorobenzyl)isothiourea. Mesh spheres represent 3D location constraints. Green: HBA. Blue: Hyd. Orange: RA. Purple: HBD. Red: +ve. Grey: excluded volume. Refer to Figure 1 for atom colour codes.

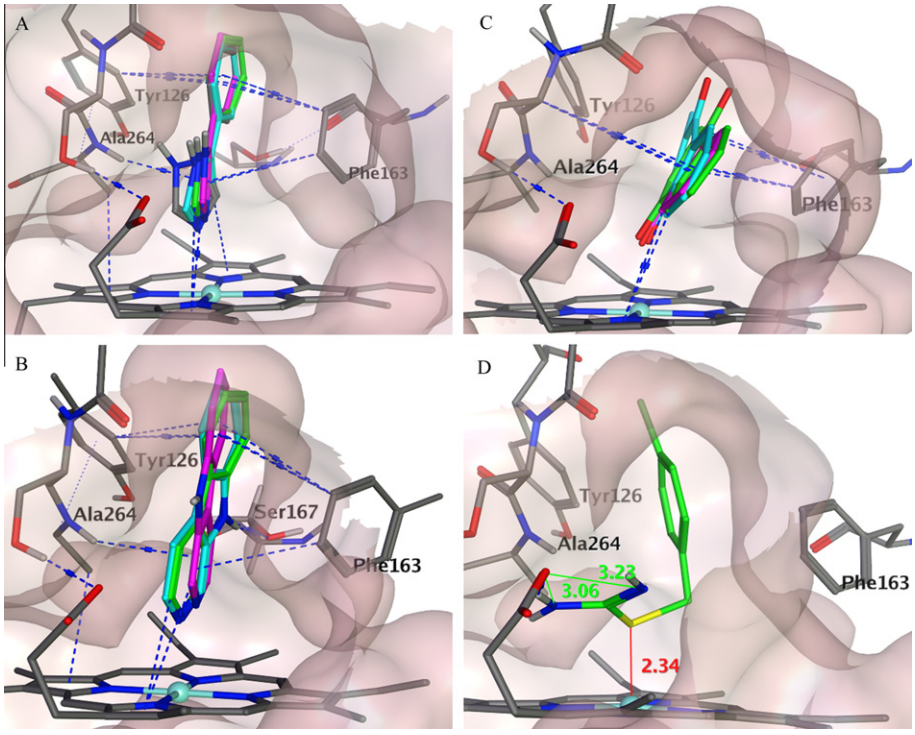

Figure 3. Docking of known inhibitors to IDO-1. (A) PI. (B) Norharman. (C) Menadione. (D) *S*-(4-Chlorobenzyl)isothiourea. Grey: crystal structure carbons. Cyan: Rohrig et al.[15] Pink: this study without cubic potential. Green: this study with cubic potential. Blue lines denote active site interactions of -0.4 kcal/mol or better.

3.2. Pharmacophore hypothesis validation

The hypotheses developed from training sets 1 and 2 gave very similar results. The complexity scores for the training sets were 11.6 and 7.7, respectively. These relatively low scores reflect the fact that the majority of IDO-1 inhibitors have few rotatable bonds. In training set 1, the top 3 hypotheses (which all had a null difference $\geqslant$40, highest being 46 with an *R* of 0.85) gave feature sets consisting of a hydrogen-bond acceptor (HBA), two hydrophobic (Hyd) features and an aromatic ring feature (RA). They also possessed 1–2 excluded volumes. The results of training set 2, however, gave hypotheses with slightly improved statistics and more feature rich pharmacophores (Table 2). The addition of extra features in the hypotheses was seen as advantageous in light of our stated goal of finding an IDO-specific pharmacophore, as a complex pharmacophore should give rise to fewer false positives and hits should possess lower off-target activity. Hypo2 from training set 2 was chosen for further work due to its good statistics and its feature richness compared to the other hypotheses.

Table 3
Comparison of docked poses with and without cubic potential

Inhibitor	Interaction	Without potential (Å)	With potential (Å)	Rohrig[15]
PI	Fe–N[a]	2.54	2.23	2.06
Menadione	Fe–O	2.81	2.22	2.13
Norharman	Fe–N	2.66	2.25	2.13
	Indolic N-Ser167	6.65	3.16	3.25
S-(4-Chlorobenzyl)isothiourea	Fe–S	2.93	2.34	Not docked
	N–COO	2.92	3.06	

[a] Crystal structure distances are 2.08 Å and 2.13 Å in chain A and B respectively.

Table 4
Twenty molecules identified from in silico screening, their fits to each pharmacophore and their Kier flexibility

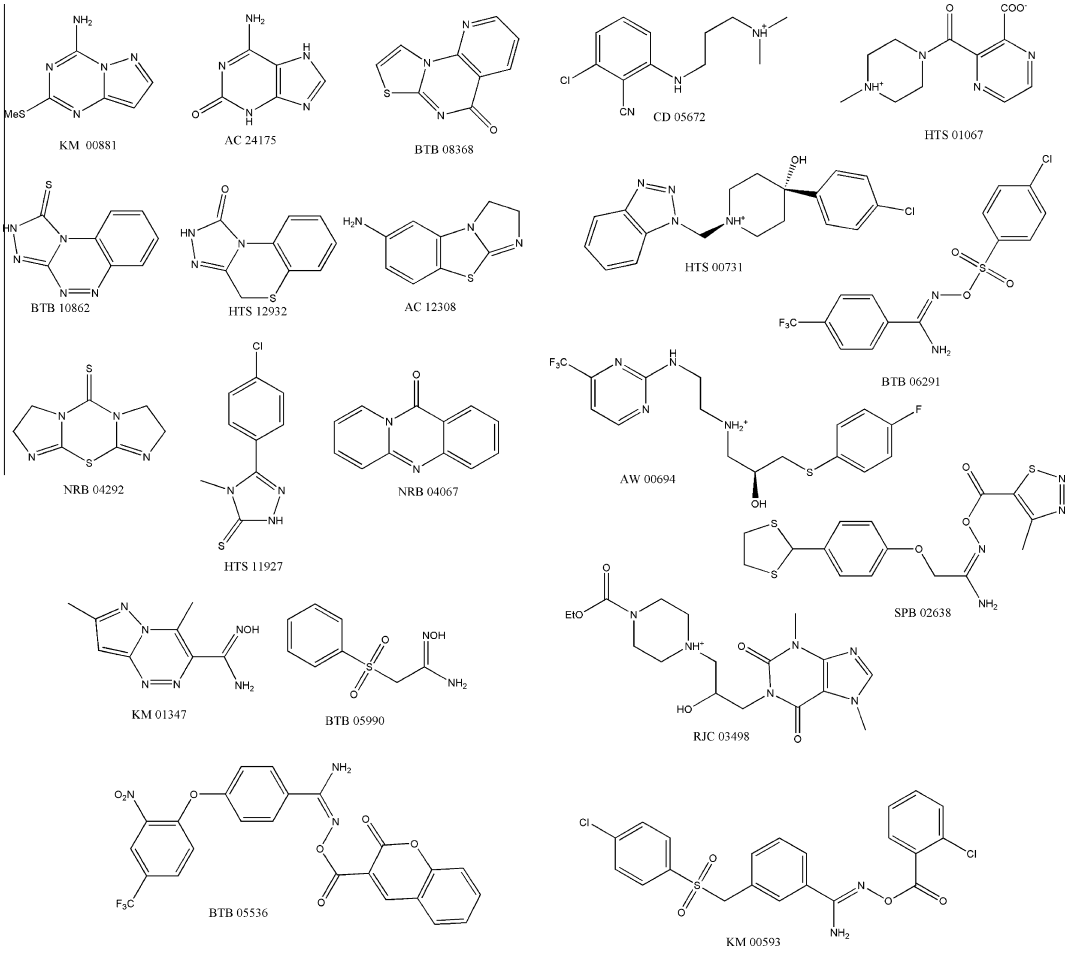

Hit	Ligand-based	PI/CHES-based	Isothiourea-based	Kier	Hit	Ligand-based	PI/CHES-based	Isothiourea-based	Kier
AC 12308	2.42	0.00	0.23	1.18	HTS 01067	2.64	2.64	2.66	2.79
AC 24175	2.62	1.42	0.00	0.63	HTS 11927	2.59	1.54	1.79	2.23
AW 00694	4.96[a]	2.45	2.40	6.48	HTS 12932	2.99	1.18	0.20	1.28
BTB 05536	3.79	3.68[a]	1.97	5.04	KM 00593	4.77[a]	2.72	2.68	6.40
BTB 05990	3.82	1.87	2.54	3.11	KM 00881	2.77	1.94	1.78	1.36
BTB 06291	4.49	1.87	2.85[a]	4.91	KM 01347	3.01	1.81	2.22	1.48
BTB 08368	2.44	1.26	0.80	1.20	NRB 04067	2.29	1.13	0.17	1.05
BTB 10862	2.90	0.86	0.43	1.08	NRB 04292	2.58	1.69	0.00	1.71
CD 05672	3.94	2.73	2.44	4.29	RJC 03498	4.38	2.91[a]	2.29	4.85
HTS 00731	4.41	1.83	2.69[a]	3.42	SPB 02638	4.42	2.52	2.63	6.56

[a] Best two fits for each pharmacophore.

3.2.1. Predictiveness of Hypo2

We used 73 IDO-1 inhibitors from the literature that were not contained in the training set, to form our test set for predictivity. Where possible, we attempted to roughly maintain the same proportions of different scaffolds between the test and training sets. The correlation (R) found was only 0.02, however, indicating that the Hypo is not quantitative. Whilst not a quantitative model, such qualitatively accurate models have been used previously with

Table 5
Population of similar molecules to those hit in the Maybridge database

Hit	Similar compounds	Hit	Similar compounds
AC 12308	2	HTS 01067	0
AC 24175	0	HTS 11927	3
AW 00694	2	HTS 12932	0
BTB 05536	1	KM 00593	10
BTB 05990	3	KM 00881	7
BTB 06291	3	KM 01347	2
BTB 08368	1	NRB 04067	0
BTB 10862	3	NRB 04292	0
CD 05672	0	RJC 03498	5
HTS 00731	0	SPB 02638	0

great success as part of a strategy for in silico screening, likely due to the models' ability to account for shape complementarity between receptor and ligand.[33–35] Results of the test set prediction can be found in the Supplementary data.

3.2.2. Features within the active site

The ligand-based hypotheses share common features, and we wished to rationalise those features within the active site. Firstly we overlayed Hypos 1–4 of training set 2 and observed that the features overlap well, including the positioning of the excluded volumes around the hydrophobic/aromatic features (Fig. 2A). We therefore propose that the hydrophobic features and excluded volumes might coincide with the aromatic cleft of the pocket, which is occupied by PI in the crystal structure, the HBA feature might represent the ligating moiety and the positive ionisable feature would interact with the propanoate arm of heme.

3.3. Receptor based pharmacophores

The crystal structure used for defining the co-crystalised pharmacophore is shown in Figure 1 and the resultant pharmacophore in Figure 2C. It consists of two HBA features, and one each of an RA and a +ve. The pharmacophore resulting from docking of *S*-(4-chlorobenzyl)isothiourea (Section 3.5) consists of one HBA, an RA and a +ve feature (Fig. 2D).

3.4. Validation of docking method

Previously, Rohrig et al. made use of a Morse-like attraction potential in order to enhance their docking procedure to heme containing enzymes, including IDO-1.[15,36] During our docking of known IDO-1 inhibitors, it was noticed that a number of potent inhibitors could not be adequately docked due to heme-ligand repulsions. In order to reduce this error, we applied a flat-bottomed cubic energy potential to these ligands and received improved results, comparable to those previously published, as shown below. As there is at present no way to determine whether a particular moiety will ligate the heme of IDO-1, this potential allowed us to perform a 'What-If' analysis of our poses, in order to see what the molecule might look like under the assumption that a given atom ligates to heme.

In order to validate our docking procedure, we re-docked the co-crystalised ligand PI into the crystal structure. We also compared our docking results of known inhibitors to those of other authors. IDO-1 heme binding poses have been published by a small number of authors, however, only Rohrig et al. have released atomic co-ordinates for comparison.[13–15] Thus, we compared our flexible docking results to those rigidly docked by Rohrig et al.[15]

The co-crystalised pose of PI was reproduced to an RMSD of 0.4 Å without the cubic potential. With the benzene rings being almost identical, most of the differences arise from the imidazole ring (Fig. 3A). This is due to repulsions from the amide proton of Ala264 of the flexible loop and repulsion from heme. The repulsion with the flexible loop could be mostly eliminated by deprotonating the amide-facing nitrogen of PI. However, with no basic residues in the active site, this seemed unlikely. Use of the cubic potential reduces both the ligation distance, and the difference in dihedral angle between the two rings, compared to the crystal structure (Fig. 3 and Table 3). By comparison, Rohrig et al. initially obtained an RMSD of 0.8 Å, which was subsequently refined to 0.3 Å via the Morse-like potential between iron and nitrogen.[36]

We further wished to test our docking method against menadione, norharman and *S*-(4-chlorobenzyl)isothiourea.[13,18,27] Menadione and norharman represent test cases for oxygen and nitrogen interactions with heme, respectively. *S*-(4-Chlorobenzyl)isothiourea, a sulfur test case, has never before been docked to IDO-1.

Poses for menadione, norhmarman and *S*-(4-chlorobenzyl)isothiourea are illustrated in Figure 3, and geometric comparisons are presented in Table 3. Menadione poses scored slightly higher when the methyl group was placed inside the active site, as has been seen previously for similar molecules.[13] Ligation through the nitrogen of norharman has been confirmed experimentally, and we received a well scored pose portraying this.[31] The indolic proton can face inwards toward the rear of the pocket and Ser167, or outwards toward the propanoate arm. For our docking without restraints, only the outward facing pose was well scored as the inward facing pose did not fit the aromatic cleft well. With use of the potential, both poses were well scored and the inward facing pose slightly more so; within H-bonding distance of Ser167's hydroxyl group.

Thus, the use of the cubic potential in our docking method gave us significantly improved results over classical docking and allowed us to obtain good agreement with both experimental and modelled data of other groups.

3.5. Docking of *S*-(4-chlorobenzyl)isothiourea and its pharmacophore

The benzylisothioureas have not previously been examined by modelling in the context of IDO-1. There has been no thorough investigation of them having a ligating effect, but they have been hypothesised to form an ionic interaction with the propanoate arm through their basic thiourea group.[18] Thus we expected to see a pose where the benzene ring was situated in the aromatic cleft and the isothiourea was interacting with the propanoate. We docked the molecule in its neutral form in order to see if a nitrogen ligation pose would appear in the absence of the restraint; no such pose eventuated. Several poses placed the benzene ring in the cleft and the thiourea group toward the propanoate arm. However, they were poorly scored, due to an ill fit with the receptor, caused by heme-sulfur repulsion. Use of the potential brought the Fe–S distance from 2.93 Å to 2.34 Å. This pose subsequently became the equal highest scored, along with another that placed the benzene ring at the outer edge of the pocket for a π-cation interaction with Arg231, and the thiourea group in close proximity to the Ser167 hydroxyl group. We do not believe this pose to be likely, however, due to the tighter packing of the benzene ring with the active site and the potential ionic interaction of the first pose (Fig. 3). Further investigation is required to ascertain the importance of the Fe–S interaction.

3.6. Database results and docking

The Ligand-based, PI/CHES-based and docked benzylisothiourea-based pharmacophores gave 5320, 1046 and 3350 (total = 9716) initial hits respectively. 61% (5911) of these hits are unique to a single pharmacophore. Known IDO-1 inhibitors or their analogues were found across the sets, including: tryptophans, benzylisothioureas, quinones, benzophenones and

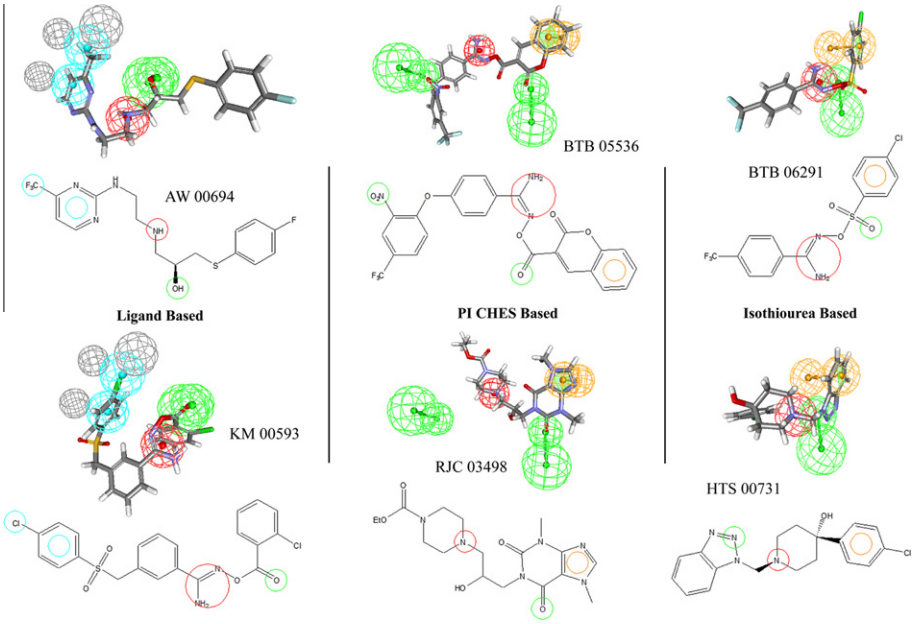

Figure 4. The two best fitting molecules from each pharmacophore are shown. Excluded volumes from the PI/CHES- and *S*-benzylisothiourea-based pharmacophores have been omitted for clarity.

phenylimidazole-like structures. Through the filtering methods and docking described, we narrowed this down to 20 molecules (9 cores and 11 extended, Table 4). These 20 molecules are generally quite unique within the database due to the high diversity of the collection (Table 5).[37] A similarity analysis, using 3 different fingerprint methods, was also conducted against 130 known IDO-1 inhibitors from scaffolds included in the training sets and those not included (such as the tryptophans, brassinins and quinones). None of the molecules displayed a Tanimoto co-efficient greater than or equal to 0.85, highlighting their uniqueness to this study. All molecules pass a Lipinski test (1 or fewer violations), and only the two largest molecules (BTB 05536 and KM 00593) fail the Oprea lead-like test, with 3 and 2 violations, respectively.[38,39] These molecules are listed in Table 4, along with their fit value to each pharmacophore and their Kier flexibility. Fit values are dependent on the complexity and features of a pharmacophore. Thus, comparison of different molecules within a pharmacophore is valid, but not across different pharmacophores. A higher fit value should indicate a more likely candidate for binding to the receptor. Additionally, a lower Kier value describes a more rigid molecule. The top two fits to each pharmacophore are shown in Figure 4.

3.7. Inhibitor testing

Of these 20 molecules, AC 24175 and KM 00881 were no longer available for purchase. The remaining 18 were obtained and tested for inhibitory activity. In an initial in vitro screening, four compounds (AC 12308, BTB 05536, KM 00593 and SPB 02638) were found to have inhibition values between 70–100% at 200 μM, with the remaining having 0–30% inhibition at the same concentration, in the presence of 200 μM L-tryptophan.

The four active compounds were tested further, with all four displaying greater activity than norharman; and the best, BTB 05536, comparable with (L-1MT). Their IC_{50} values are given in Table 6.

The potency of these inhibitors are equal to, or better than, those previously identified as initial lead compounds from in silico screening against IDO-1, and are of a potency expected from an initial virtual screen.[15,40] AC 12308 is a 'core' molecule, whilst the remaining three are found in the extended molecules category, and interestingly possess a novel esterimidamide group linking aromatic rings, which suggests this as an important moiety for these molecules. By contrast, BTB 06291 contains a sulfonate mimic of this, but was not active (Table 3). It is worth noting that BTB 05536 was highest ranked in the PI/CHES based pharmacophore, KM 00593 was second highest ranked in the ligand-based pharmacophore and that SPB 02638 was also highly ranked by each pharmacophore. AC 12308, whilst not highly ranked in the pharmacophores due to its simplicity, nonetheless was able to be identified due to the additional filtering and docking methods employed.

Table 6
Inhibitory values of selected compounds.

Inhibitor	IC_{50} (SD[c]) (μM)
AC 12308[a]	50 (1.4)
BTB 05536[b]	20 (6)
KM 00593[b]	60 (6)
SPB 02638[b]	50 (7)
L-1MT	10 (4)
Norharman	90 (7)

[a] Kyn determined by HPLC.
[b] Kyn determined by Ehrlich's reagent.
[c] Standard deviation.

Our hit rate for this study, based on an IC_{50} lower than 200 μM, is 14% (1/7) for core molecules and 27% (3/11) for extended molecules. These are comparable to hit rates of other published virtual screening studies.[34] An IC_{50} below 200 μM was deemed appropriate for the identification of new structural archetypes, within the context of the potency of known IDO-1 inhibitors. The use of multi-step in silico screening methods is becoming more commonplace within the literature as an efficient means of high-throughput in silico screening.[33,41,42]

3.8. Docking of active hits

Docking poses of the four active molecules are given in Figure 5. For AC 12308, ligation through the imino nitrogen allowed for the

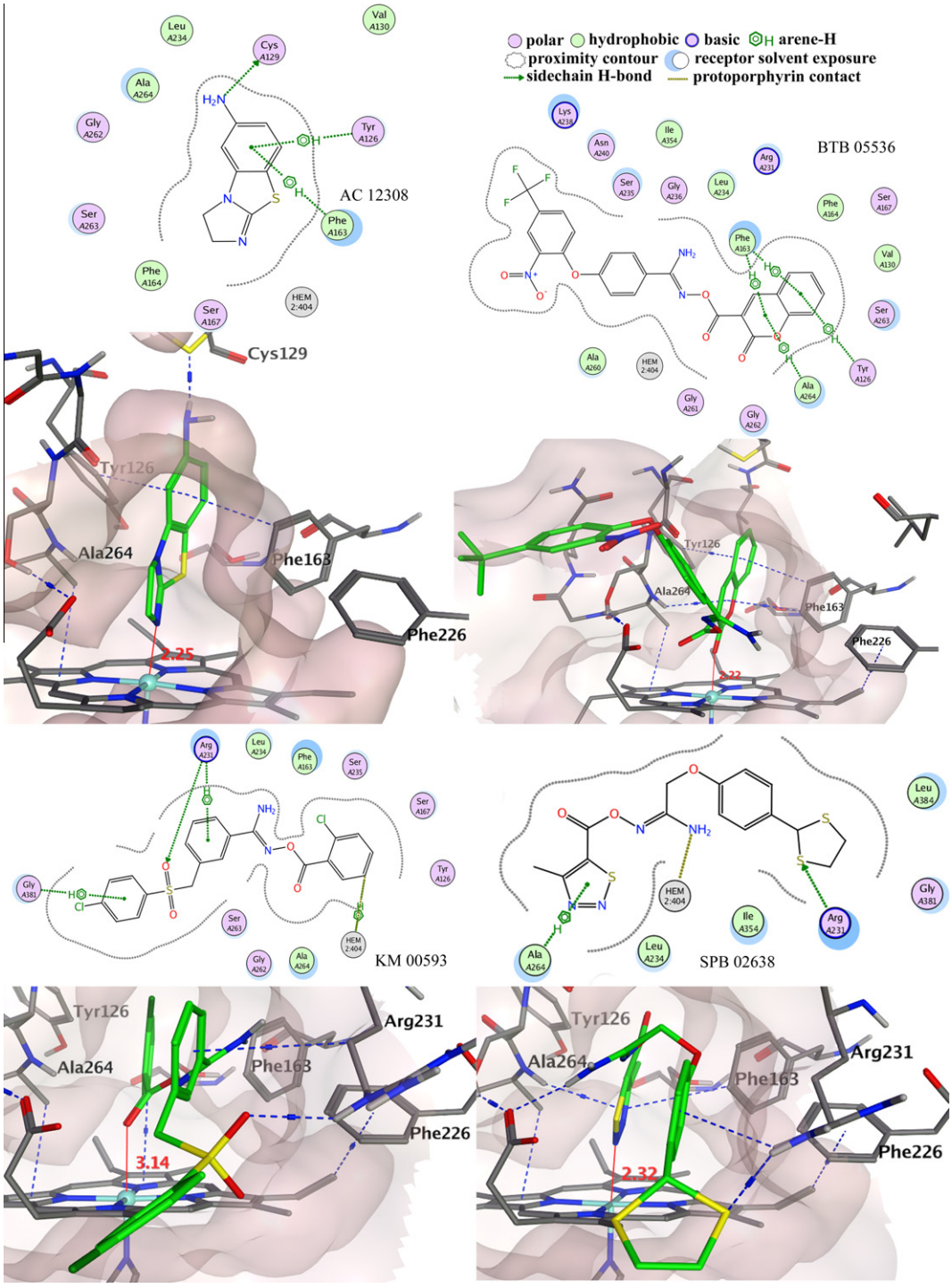

Figure 5. Proposed binding poses for AC 12308, BTB 05536, KM 00593 and SPB 02638. Broken lines indicate an active site interaction of −0.4 kcal/mol or better.

best fit in the aromatic cleft and brought the aromatic amine to within H-bonding distance of Cys129. The next best pose had ligation occurring through the sulfur, resulting in a slightly inferior fit to the aromatic cleft and loss of the Cys129 interaction. Neither binding mode can be eliminated for AC 12308. In both cases, the tolerance of the five membered ring could allow for modification of the molecule to extend out from the active site in future SAR work. Such small molecules, possessing good ligand efficiency, are often good starting points for drug optimisation studies, especially when a clearly defined path is available; such as that provided by crystal structures, and in this case, our extended molecules.[43]

BTB 05536 may bind to heme through either the lactone or the ester moiety to give two similar poses. Use of the lactone carbonyl is shown. This allows for π-proton interactions with the rings of the chromene system and Tyr126, Phe163 and Ala264. The amine portion points toward the aromatic surface created by Phe163 and Phe226 for probable π-proton interactions. We also tested the ester carbonyl as the ligating atom. In this instance the lactone carbonyl moved towards Ser167 and the nitrobenzene moved

slightly closer to Arg231, at the cost of causing some minor ring strain in the pyranone ring.

KM 00593 can also adopt a pose similar to BTB 05536, with heme ligation through the ester carbonyl and the amine portion pointed towards the surface created by Phe163 and Phe226. This allows for an H-bonding opportunity between Arg231 and the sulfone. Alternatively, the sulfone may reside above the heme, with one oxygen pointed towards the iron and another within H-bonding distance of the Ala264 amide proton. The amine of the imidamide is then free to interact with the propanoate arm, while Arg231 forms a π-stacking interaction with the ester and benzene ring. The 4-chlorobenzene sulfinic and sulfonic acids have both been reported as having poor inhibition properties, as did BTB 05990 and 06291 in this study.[18] This would argue against a sulfinic binding pose.

SPB 02638 could potentially ligate through any of the thiadiazole heteroatoms, the esterimidamide and/or the dithiolane ring. The pose interacting through the nitrogen of the thiadiazole ring is proposed in Figure 5, as this led to the highest number of polar interactions. This allows for a π-proton interaction between Arg231 and the benzene ring and H-bonding interactions between the dithiolane ring and Arg231, as well as between the amine and propanoate arm. The thiadiazole ring additionally forms π-proton and π–π interactions with Ala264 and Phe163. Another possible pose was to mimic the pose of BTB 05536 and KM 00593 by having the carbonyl of the esterimidamide ligate to iron and the amino portion in the aromatic surface created by Phe163 and Phe226, at the cost of any interaction with Arg231. A third pose may be to have the dithiolane ring ligating to heme. Such a pose has the amine of the esterimidamide sitting above the propanoate arm, the benzene ring with edge-on interactions to Phe163 and Phe226 and the thiadiazole ring just outside of H-bonding distance of the Gly261 amide proton.

Alternate poses are provided in the Supplementary data.

4. Conclusion

The in silico database searches with three pharmacophores developed from ligand-, crystal structure-, and docking-based approaches, coupled with refinement of hits through Kier flexibility scoring and 'What-If' docking analysis, has enabled the retrieval of four unique and novel inhibitors of IDO-1 from in vitro testing of only 18 compounds. Further, the four active compounds show activities comparable to the known IDO inhibitors, norharman and 1-methyl-L-tryptophan. The low micromolar potency of these inhibitors is comparable with other initial lead compounds discovered for IDO-1. Docking poses have been derived to account for the potential binding modes of each of these novel IDO-1 inhibitors.

The compounds BTB 05536, KM 00593 and SPB 02638, which possess a novel structural element, an esterimidamide linker between two aromatic regions, appear to have much greater interactions with the active site compared to many of the simple IDO-1 inhibitors reported to date. The smaller scaffold seen in AC 12308 shows promise for further extension into other regions of the active site.

Acknowledgements

Financial support for this work was provided by the National Health and Medical Research Council (NHMRC grant 281505).

Supplementary data

Supplementary data associated with this article can be found, in the online version, at doi:10.1016/j.bmc.2011.10.068.

References and notes

1. Lewis-Ballester, A.; Batabyal, D.; Egawa, T.; Lu, C.; Lin, Y.; Marti, M. A.; Capece, L.; Estrin, D. A.; Yeh, S. R. *PNAS* **2009**, *106*, 17371–17376.
2. Ball, H. J.; Sanchez-Perez, A.; Weiser, S.; Austin, C. J. D.; Astelbauer, F.; Miu, J.; McQuillan, J. A.; Stocker, R.; Jermiin, L. S.; Hunt, N. H. *Gene* **2007**, *396*, 203–213.
3. Rafice, S. A.; Chauhan, N.; Efimov, I.; Basran, J.; Raven, E. L. *Biochem. Soc. Trans.* **2009**, *37*, 408–412.
4. Sono, M.; Roach, M. P.; Coulter, E. D.; Dawson, J. H. *Chem. Rev.* **1996**, *96*, 2841–2888.
5. Batabyal, D.; Yeh, S.-R. *J. Am. Chem. Soc.* **2007**, *129*, 15690–15701.
6. Guallar, V.; Wallrapp, F. H. *Biophys. Chem.* **2010**, *149*, 1–11.
7. Chung, L. W.; Li, X.; Sugimoto, H.; Shiro, Y.; Morokuma, K. *J. Am. Chem. Soc.* **2010**, *132*, 11993–12005.
8. Pearson, J. T.; Siu, S.; Meininger, D. P.; Wienkers, L. C.; Rock, D. A. *Biochemistry* **2010**, *49*, 2647–2656.
9. Sugimoto, H.; Oda, S.-I.; Otsuki, T.; Hino, T.; Yoshida, T.; Shiro, Y. *PNAS* **2006**, *103*, 2611–2616.
10. Munn, D. H.; Zhou, M.; Attwood, J. T.; Bondarev, I.; Conway, S. J.; Marshall, B.; Brown, C.; Mellor, A. L. *Science* **1998**, *281*, 1191–1193.
11. Uyttenhove, C.; Pilotte, L.; Theate, I.; Stroobant, V.; Colau, D.; Parmentier, N.; Boon, T.; Eynde, B. J. V. D. *Nat. Med.* **2003**, *9*, 1269–1274.
12. Muller, A. J.; DuHadaway, J. B.; Donover, P. S.; Sutanto-Ward, E.; Prendergast, G. C. *Nat. Med.* **2005**, *11*, 312–319.
13. Kumar, S.; Malachowski, W. P.; DuHadaway, J. B.; LaLonde, J. M.; Carroll, P. J.; Jaller, D.; Metz, R.; Prendergast, G. C.; Muller, A. J. *J. Med. Chem.* **2008**, *51*, 1706–1718.
14. Kumar, S.; Jaller, D.; Patel, B.; LaLonde, J. M.; DuHadaway, J. B.; Malachowski, W. P.; Prendergast, G. C.; Muller, A. J. *J. Med. Chem.* **2008**, *51*, 4968–4977.
15. Röhrig, U. F.; Awad, L.; Grosdidier, A. L.; Larrieu, P.; Stroobant, V.; Colau, D.; Cerundolo, V.; Simpson, A. J. G.; Vogel, P.; Van den Eynde, B. T. J.; Zoete, V.; Michielin, O. *J. Med. Chem.* **2010**, *53*, 1172–1189.
16. http://clinicaltrials.gov/. (last accessed: 14/10/2011).
17. Peterson, A. C.; Migawa, M. T.; Martin, M. J.; Hamaker, L. K.; Czerwinski, K. M.; Zhang, W.; Arond, R. A.; Fisette, P. L.; Ozaki, Y.; Will, J. A.; Brown, R. R.; Cook, J. M. *Med. Chem. Res.* **1994**, *3*, 531–544.
18. Matsuno, K.; Takai, K.; Isaka, Y.; Unno, Y.; Sato, M.; Takikawa, O.; Asai, A. *Bioorg. Med. Chem. Lett.* **2010**, *20*, 5126–5129.
19. http://www.daylight.com/dayhtml_tutorials/languages/smarts/index.html#INTRO (last accessed: 14/10/2011).
20. Hall, L. H.; Kier, L. B. *The Molecular Connectivity Chi Indexes and Kappa Shape Indexes in Structure-Property Modeling*; John Wiley & Sons, Inc.: Hoboken, NJ, USA, 2007.
21. Pyykkö, P.; Atsumi, M. *Chemistry–A European Journal* **2009**, *15*, 186–197.
22. Austin, C. J. D.; Mizdrak, J.; Matin, A.; Sirijovski, N.; Kosim-Satyaputra, P.; Willows, R. D.; Roberts, T. H.; Truscott, R. J. W.; Polekhina, G.; Parker, M. W.; Jamie, J. F. *Prot. Expr. Purif.* **2004**, *37*, 392–398.
23. Austin, C.; Astelbauer, F.; Kosim-Satyaputra, P.; Ball, H.; Willows, R.; Jamie, J.; Hunt, N. *Amino Acids* **2009**, *36*, 99–106.
24. Sono, M. *Biochemistry* **1990**, *29*, 1451–1460.
25. Yue, E. W.; Douty, B.; Wayland, B.; Bower, M.; Liu, X.; Leffet, L.; Wang, Q.; Bowman, K. J.; Hansbury, M. J.; Liu, C.; Wei, M.; Li, Y.; Wynn, R.; Burn, T. C.; Koblish, H. K.; Friedman, J. S.; Metcalf, B.; Scherle, P. A.; Combs, A. P. *J. Med. Chem.* **2009**, *52*, 7364–7367.
26. Peterson, A. C.; Loggia, A. J. L.; Hamaker, L. K.; Arend, R. A.; Fisette, P. L.; Ozaki, Y.; Will, J. A.; Brown, R. R.; Cook, J. M. *Med. Chem. Res.* **1993**, *3*, 473–482.
27. Eguchi, N.; Watanabe, Y.; Kawanishi, K.; Hashimoto, Y.; Hayaishi, O. *Arch. Biochem. Biophys.* **1984**, *232*, 602–609.
28. Southan, M.; Truscott, R.; Jamie, J.; Pelosi, L.; Walker, M.; Maeda, H.; Iwamoto, Y.; Tone, S. *Med. Chem. Res.* **1996**, *6*, 343–352.
29. Gaspari, P.; Banerjee, T.; Malachowski, W. P.; Muller, A. J.; Prendergast, G. C.; DuHadaway, J.; Bennett, S.; Donovan, A. M. *J. Med. Chem.* **2006**, *49*, 684–692.
30. Carr, G.; Chung, M. K. W.; Mauk, A. G.; Andersen, R. J. *J. Med. Chem.* **2008**, *51*, 2634–2637.
31. Sono, M.; Cady, S. G. *Biochemistry* **1989**, *28*, 5392–5399.
32. Albert, A.; Goldcare, R.; Phillips, J. *J. Chem. Soc. (Resumed)* **1948**, *455*, 2240–2249.
33. Drwal, M. N.; Agama, K.; Wakelin, L. P. G.; Pommier, Y.; Griffith, R. *PLoS ONE* **2011**, *6*, e25150.
34. Stoddart, E. S.; Senadheera, S.; MacDougall, I. J. A.; Griffith, R.; Finch, A. M. *PLoS ONE* **2011**, *6*, e19695.
35. Kortagere, S.; Krasowski, M. D.; Ekins, S. *Trends. Pharmacol. Sci.* **2009**, *30*, 138–147.
36. Röhrig, U. F.; Grosdidier, A.; Zoete, V.; Michielin, O. *J. Comp. Chem.* **2009**, *30*, 2305–2315.
37. McGregor, M. J.; Pallai, P. V. *J. Chem. Inf. Comput. Sci.* **1997**, *37*, 443–448.
38. Lipinski, C. A.; Lombardo, F.; Dominy, B. W.; Feeney, P. J. *Adv. Drug Del. Rev.* **1997**, *23*, 3–25.
39. Oprea, T. I. *J. Comput. Aided Mol. Des.* **2000**, *14*, 251–264.
40. Klebe, G. *Drug Discovery Today* **2006**, *11*, 580–594.
41. Talevi, A.; Gavernet, L.; Bruno-Blanch, L. E. *Curr. Comput. Aided Drug Des.* **2009**, *5*, 23–37.
42. Hein, M.; Zilian, D.; Sotriffer, C. A. *Drug Discov. Today Technol.* **2010**, *7*, e229–e236.
43. Erlanson, D. A.; McDowell, R. S.; O'Brien, T. *J. Med. Chem.* **2004**, *47*, 3463–3482.